A Summary of Precipitation Characteristics from the 2006–11 Northern Australian Wet Seasons as Revealed by ARM Disdrometer Research Facilities (Darwin, Australia)

SCOTT E. GIANGRANDE AND MARY JANE BARTHOLOMEW

Environmental and Climate Sciences Department, Brookhaven National Laboratory, Upton, New York

MICK POPE

Bureau of Meteorology Training Center, Bureau of Meteorology, Melbourne, Victoria, Australia

SCOTT COLLIS

Environmental Sciences Division, Argonne National Laboratory, Argonne, Illinois

MICHAEL P. JENSEN

Environmental and Climate Sciences Department, Brookhaven National Laboratory, Upton, New York

(Manuscript received 8 July 2013, in final form 12 December 2013)

ABSTRACT

The variability of rainfall and drop size distributions (DSDs) as a function of large-scale atmospheric conditions and storm characteristics is investigated using measurements from the Atmospheric Radiation Measurement Program (ARM) facility at Darwin, Australia. Observations are obtained from an impact disdrometer with a near continuous record of operation over five consecutive wet seasons (2006–11). Bulk rainfall characteristics are partitioned according to diurnal accumulation, convective and stratiform precipitation classifications, objective monsoonal regime, and MJO phase. Findings support previous Darwin studies suggesting a significant diurnal and DSD parameter signal associated with both convective–stratiform and wet season monsoonal regime classification. Negligible MJO phase influence is determined for cumulative disdrometric statistics over the Darwin location.

1. Introduction

Accurate precipitation measurements benefit a wealth of climate, atmospheric, and hydrologic applications. For the representation of deep convection and its influence on precipitation and cloud system diabatic heating, improvements to larger-scale convective parameterizations and more explicit storm-scale model treatments argue for new observational constraints that better elucidate complex interactions of convective dynamics and precipitation microphysics (e.g., Milbrandt and Yau 2005; Stephens 2005; Jakob 2010; Del Genio 2012; Varble et al. 2011). Constructing useful observational metrics for model evaluation and advancement has reemphasized the importance for attributing bulk cloud and precipitation properties to associated environmental forcing. For climate-critical regions, particularly the tropical western Pacific, this sort of model-observational dataset construction is challenging as a consequence of prohibitive costs for extended, well-sampled field deployments and the maintenance of observational platforms in remote or oceanic locations (e.g., Webster and Lukas 1992; Holland et al. 1986; Keenan et al. 1989, 2000; Mather et al. 1998; Lau et al. 2000; Blossey et al. 2007; May et al. 2008; Long et al. 2013).

Although not necessarily remote, the northern Australia region shares in several of the challenges faced when characterizing tropical precipitation and its interconnections to atmospheric processes at weather and

Corresponding author address: Scott Giangrande, Environmental and Climate Sciences Department, Brookhaven National Laboratory, Building 490D, Bell Ave., Upton, NY 11973.
E-mail: scott.giangrande@bnl.gov

DOI: 10.1175/JAMC-D-13-0222.1

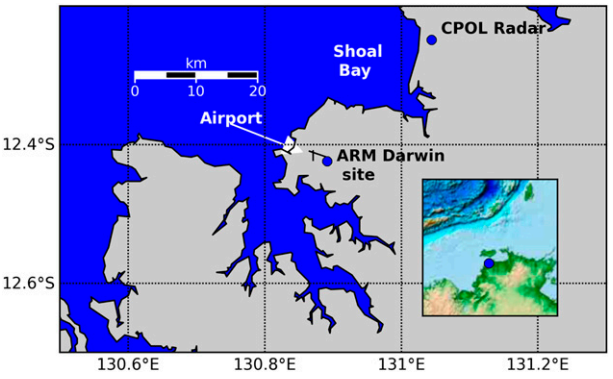

FIG. 1. Map showing the location of the ARM TWP Darwin site.

climate scales. Annual precipitation in northern Australia is highly seasonal, a majority of the variability being linked with the onset of the summer monsoon (e.g., Drosdowsky 1996). Defining the wet season to include the period between approximately September through April, this time window accounts for nearly all measurable rainfall events over the region (e.g., Nicholls et al. 1982; Nicholls 1984). Embedded within this strong monsoonal signal, recent tropical western Pacific observational studies have sought to improve integrated microphysical–dynamic–thermodynamic insight through better partitioning of 1) modes favorable for shallow to deep convection, for example, so-called active and break monsoonal periods (e.g., Holland 1986; Keenan and Carbone 1992; Rosenfeld et al. 1993; Drosdowsky 1996; May and Ballinger 2007; Kumar et al. 2013), 2) the interseasonal Madden–Julian oscillation (MJO) influences (e.g., Wheeler and Hendon 2004, hereinafter WH; Kozu et al. 2005; Lau and Wu 2010), 3) diurnal variability within monsoonal regimes (e.g., Keenan et al. 1989; Ushiyama et al. 2009; Kumar et al. 2013), and 4) convective–stratiform precipitation segregations (e.g., Keenan et al. 1989; Steiner et al. 1995; Tokay and Short 1996; Atlas et al. 1999; Maki et al. 2001; Penide et al. 2013).

This study explores rainfall and drop size distribution (DSD) characteristics contingent on several known seasonal and shorter regime behaviors from a multiyear archive collected by the U.S. Department of Energy's Atmospheric Radiation Measurement Program (ARM) climate research facility at Darwin, Australia (Fig. 1; e.g., Stokes and Schwartz 1994; Ackerman and Stokes 2003; Long et al. 2013; Mather and Voyles 2013). The current summary builds on existing tropical western Pacific (TWP) and northern Australian disdrometric efforts and is intended as additional reference for ongoing Darwin multisensor, multiparameter radar studies toward improved climate modeling (e.g., Bringi et al. 2009; Thurai et al. 2010; Kumar et al. 2013; Penide et al. 2013; Dolan et al. 2013). The ARM TWP collection period provided for this study overlaps with several regional tropical modeling campaigns including the Year of Tropical Convection (e.g., Waliser et al. 2012).

The paper has been organized as follows: The ARM surface instrumentation package and methodologies for this study are provided in section 2. Section 3 provides the results for this dataset. A discussion and summary of key findings are provided in sections 4 and 5.

2. Dataset and methodology

a. *The ARM Joss–Waldvogel disdrometer observations and processing*

The primary precipitation observations for this study are obtained using the Joss–Waldvogel disdrometer (JWD; Joss and Waldvogel 1967) model RD-80 that experienced negligible collection downtime during the period from September 2006 to May 2011 covering five Darwin wet seasons. Measurements of the DSD and its estimated parameters are collected at 1-min aggregation windows and sampled at 5-min aggregation windows for this study for improved reliability of the ARM records. Impact disdrometers are susceptible to several known system sampling limitations (e.g., Sheppard and Joe 1994) and include possible wind-related undercatchment (e.g., Nešpor and Sevruk 1999; Duchon and Essenberg 2001), quantization (binning; e.g., Marzuki et al. 2010), and instantaneous measurement noisiness from physical process variability (e.g., Lee and Zawadzki 2005). These limitations have impacts on functional-form DSD parameter fits (e.g., Smith et al. 2009, Cao and Zhang 2009) and several direct measurements. Routinely measured JWD quantities in moderate to heavier rainfall, in particular those quantities related to the higher DSD moments over an extended dataset, are still useful if appropriately characterized and aggregated.

Emphasis for this study is on the accumulated rainfall and rainfall intensity parameters from these ARM systems. The primary measurements include the rainfall rate R (mm h^{-1}) and rainwater content W (g m^{-3}) following definitions and considerations standard to impact disdrometric work (e.g., Tokay and Short 1996; Leinonen et al. 2012) and parameter retrievals following functional fits for drop fall speeds (e.g., Gunn and Kinzer 1949) and standard dead time corrections (Sheppard and Joe 1994). This includes additional ARM JWD fields for the measured median volume drop size D_0 (mm), the mass-weighted mean diameter D_m (mm), and radar reflectivity factor Z (dBZ) following Rayleigh theory and a spherical drop assumption. Parameters of a gamma-fit (complete) DSD of the form

TABLE 1. Darwin JWD disdrometer wet season rainfall accumulation summary including fractional convective rainfall total according to Bringi et al. (2009) segregation. Fractional DW-active and ME-break monsoon totals are according to Pope et al. (2009) segregations. The approximate monsoon onset date is according to a rainfall-based definition, e.g., Smith et al. (2008).

Wet season	2006/07	2007/08	2008/09	2009/10	2010/11
Rainfall total (mm)	1567	1824	1528	1950	2694
% convective	66	68	69	72	62
% DW-active	26	23	24	26	54
% ME-break	47	37	37	30	37
Monsoon onset date	30 Dec	25 Dec	10 Dec	12 Dec	11 Dec

$N(D) = N_0 D^{\mu} \exp(-\Lambda D)$ having equivalent volume diameter D with number concentration N_0 ($\text{mm}^{-1}\,\text{m}^{-3}$), shape parameter μ, and slope parameter Λ (mm^{-1}) are also routinely calculated following existing JWD disdrometer methods of higher moments (second, fourth, and sixth moment method) of the observed DSDs (e.g., Cao and Zhang 2009).

Calculations for a normalized DSD intercept parameter Nw have been adapted following Testud et al. (2001) among several others and implemented for this study in order to adopt a convective–stratiform partitioning scheme based on disdrometer and additional Darwin profiler observations (Bringi et al. 2002, 2003, 2009). In following such references, the mass-weighted diameter is calculated as

$$D_m = E(D^4)/E(D^3), \tag{1}$$

where E stands for expectation. Similarly, the liquid water content W is calculated as

$$W = \frac{\pi}{6}\rho_w E(D^3), \tag{2}$$

where ρ_w is the density of water. The expressions in (1) and (2) are used to compute an intercept parameter N_w ($\text{mm}^{-1}\,\text{m}^{-3}$) as

$$N_w = \frac{4^4}{\pi\rho_w}\left(\frac{W}{D_m^4}\right). \tag{3}$$

For estimates of D_0 that are difficult to calculate directly and accurately from binned JWD observations, the gamma DSD method of moments parameter fits were utilized given an expression $D_0 = (3.67 + \mu)/\Lambda$. This approach to estimating D_0 may experience uncertainty in response to known JWD small drop sampling limitations, potential truncation issues and the integrity of these retrievals in lighter rainfall $< 5\,\text{mm}\,\text{h}^{-1}$ (e.g., Cao and Zhang 2009). It is noted that D_0 may also be estimated from D_m and for a gamma distribution these parameters are related according to $D_m = D_0(4 + \mu)/(3.67 + \mu)$ (e.g., Testud et al. 2001). These estimates compared well with those determined from the DSD parameter fits (not shown).

b. Extended Darwin dataset

Table 1 contains a summary of wet season rainfall characteristics for the monsoon seasons sampled by the ARM Darwin disdrometer. This summary includes the rainfall total, a rainfall-based onset date (accumulated rainfall is equal to 15% of the seasonal total; e.g., Smith et al. 2008), and the fractional total of precipitation attributed to convective precipitation following the disdrometric multiparameter analysis approach as in Bringi et al. (2009). Details for this particular method of disdrometric convective–stratiform analysis will be discussed in later sections. Similarly, Table 1 includes an additional disdrometer breakdown for ''deep west'' (DW) or active monsoon and ''moist east'' (ME) or break monsoon regimes following Pope et al. (2009) classifications to be discussed in later sections.

For an additional quality control check, JWD accumulations were compared to the set of 1-min resolution Novalynx tipping-bucket rain gauges (model 260–2500E-12) at the ARM Darwin location. The primary rain gauge system was collocated with the JWD at the ARM Darwin location; the other ARM system was available as reference at close distance (within 50 m). As demonstrated by the 2008/09 wet season example in Fig. 2, rainfall captured by both instrument types when they are simultaneously functioning agreed to within 10% for all wet seasons presented in this study. This provides some confidence in the JWD as a standalone platform, despite known differences between these measurements and rainfall capture capabilities (e.g., Nešpor and Sevruk 1999; Habib et al. 2001). The exclusion of light rain DSDs having rainfall rates $< 0.5\,\text{mm}\,\text{h}^{-1}$ and/or low drop counts (under 20 drops) was associated with the loss of approximately 1%–2% of the total accumulation during Darwin wet seasons.

According to a standard rainfall-based definition (e.g., Nicholls 1984; Smith et al. 2008), monsoon onsets favored

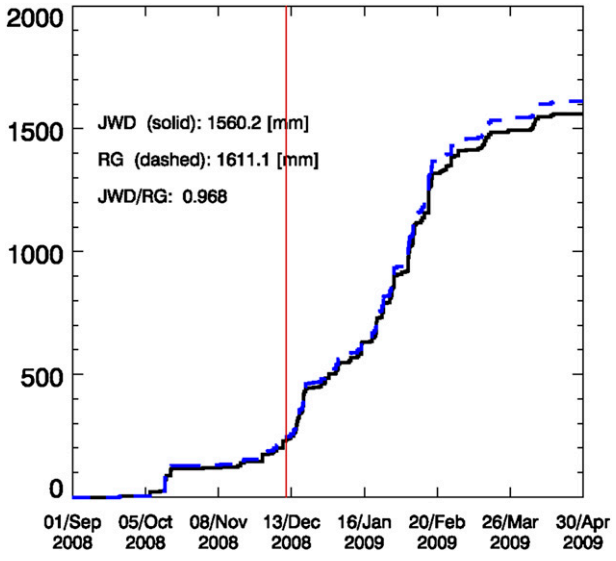

FIG. 2. Plot of the accumulated rainfall for the Darwin disdrometer (solid) and rain gauge (dashed blue) for the 2008/09 wet season. Red line indicates an approximate monsoon onset date on which 15% of the season total rainfall was reached.

mid- to late December and were often associated with a singular intense rainfall event. The average rainfall accumulation over the five wet seasons exceeded 1900 mm at this disdrometer system. However, this average includes the record-breaking 2010/11 wet season that featured over 1000 mm of additional accumulation above this previous climatological Darwin average (~1650 mm; e.g., Smith et al. 2008). Totals during the 2010/11 wet season were likely enhanced by two unique contributions: the strong La Niña in the tropical Pacific Ocean and the landfall of Tropical Cyclone (TC) Carlos. The 16 February 2011 TC Carlos event shattered previous 24-h rainfall records for Darwin.

c. *Precipitation regimes for Darwin*

As highlighted by the 2010/11 Darwin wet season, many factors that include larger-scale coupled ocean–atmospheric La Niña and individual extreme event influences can contribute to wet season precipitation totals. For the Darwin region, diurnal variations have been documented for rain gauge and radar efforts to show specific characteristic features (e.g., Keenan et al. 1989). In addition to emphasizing diurnal rainfall characteristics over this ARM location, this study aims to contribute additional insights from these ARM disdrometers toward additional regime partitioning models as described in the following sections. Previous Darwin studies have documented competing factors when reconciling the role of larger-scale regimes on the properties of convective clouds. As one example, Kumar et al. (2013) indicate that the majority of land-based precipitation observed during break monsoonal conditions over Darwin are cells that initiate in the afternoon by seabreeze processes. For these conditions, the study reports markedly different radar-based storm properties (e.g., radar echo-top height, cell motion) as compared to those properties associated with cells initiating over the ocean under the same larger-scale regime. Similarly, Thurai et al. (2010) use radar-based DSD retrievals to report distinct DSD separations between ocean- and land-based convective and stratiform regimes, highly contingent on the larger-scale monsoonal regime. Exotic DSD characteristics may be specific to select sampling windows and/or convective types (e.g., isolated convective cells, squall lines, as in Rosenfeld et al. 1993; Cifelli et al. 2000; Maki et al. 2001). For modelers to benefit from insights obtained using a single location (representativeness), we caution that bulk regime characterization found in this study that includes rainfall and DSD parameters must be carefully interpreted in light of these forms of competing considerations.

Heavier precipitation over Darwin is also occasionally linked to severe tropical systems. Long-term studies from Dare et al. (2012) indicate that approximately 10% of the Darwin seasonal rainfall may be attributed to significant tropical events, although this study suggests the ARM Darwin location should experience substantial interannual variability on those amounts. Previous studies indicate these systems may contain unique DSD characteristics consistent only within the macrophysical structures unique to these systems (e.g., rainbands, eyewall, as in Ulbrich and Lee 2002; Tokay et al. 2008). We note that the ARM dataset includes DSDs obtained during the record-setting TC Carlos event from the 2010/11 wet season, as well as a significant TC Helen event that formed over Darwin during the 2007/08 wet season. However, the current analysis does not explicitly address the separate DSD characteristics (and potential for mischaracterization of bulk regime influence) associated with these tropical systems, having contribution to the total Darwin precipitation over the 5-yr window less than 5%.

Figure 3 provides separate realizations for each of the five Darwin wet seasons explored for this study. These summaries are plotted in terms of the JWD 24-h (daily) total rainfall (black trace) as well as additional monsoonal regimes (following Pope et al. 2009) and MJO phase (following WH) to be discussed in additional detail throughout this section. These realizations emphasize the organization of the typical northern Australia wet season and its evolution; however, they reinforce the known complexity of each. For example, all wet season realizations in Fig. 3 exhibit an overarching progression

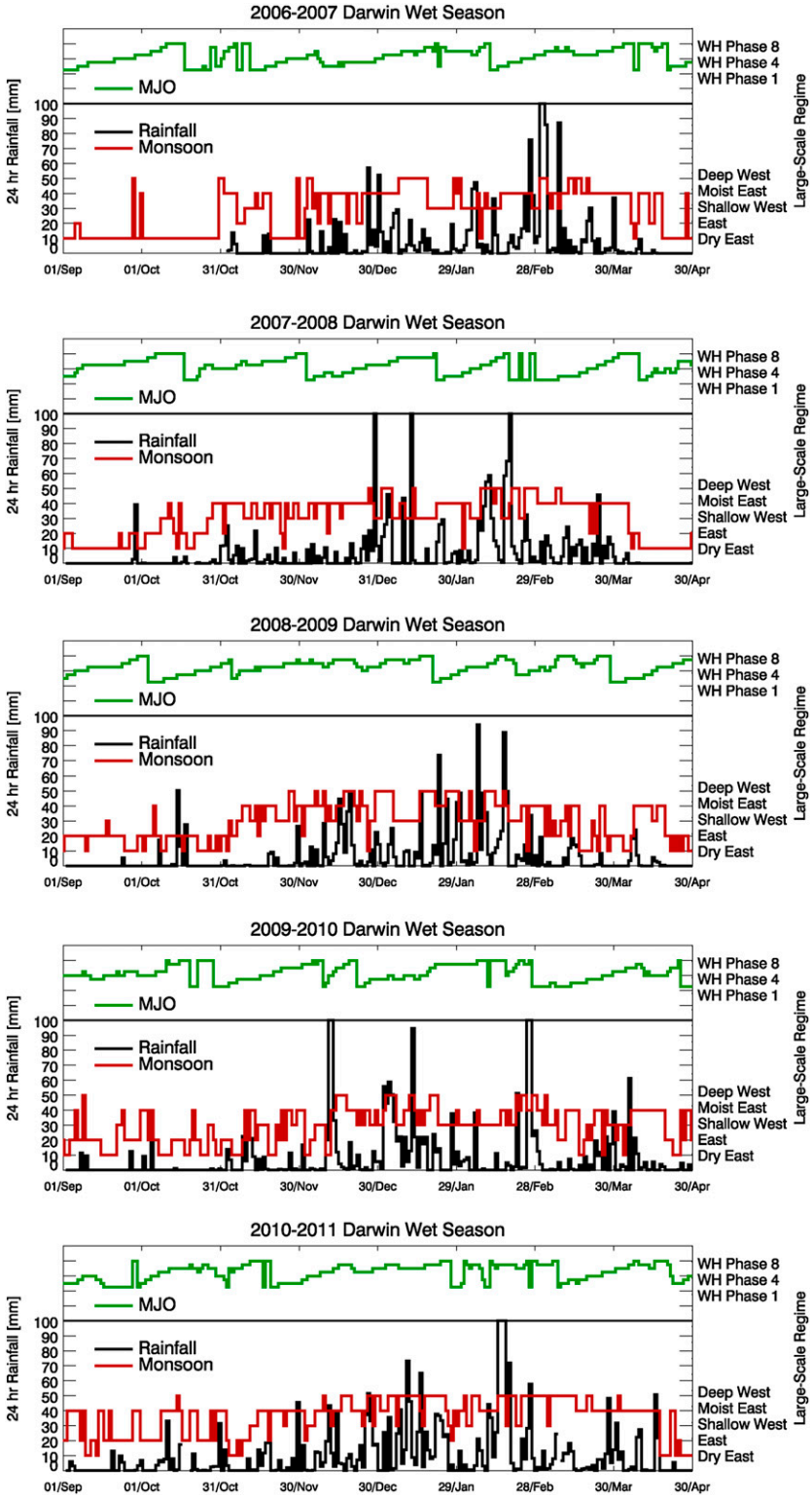

FIG. 3. Time series realizations for each wet season over the Darwin location. 24-h rainfall totals (black trace) correspond to the left *y* axis scales. Right *y* axis includes the WH MJO phase (green trace, upper subset from WH phase 1 to WH phase 8) and Pope et al. (2009) larger-scale monsoon (red trace, lower subset from categories DE to DW) regime breakdown cycles.

toward monsoonal DW and ME modes (red trace) by months January and February that have been shown to be well associated with ''active'' shallow convective environments and ''break/build-up'' deep convective periods (e.g., Pope et al. 2009). Yet, it is clear these Darwin monsoonal regimes may be convolved with multiple MJO cycles throughout the course of any wet season (Fig. 3, green trace) as well as heavier rainfall episodes having no presumed preferential MJO or monsoonal phasing (e.g., tropical cyclone events).

1) CONVECTIVE–STRATIFORM PARTITIONING

Model precipitation is often segregated into bulk convective or widespread stratiform components, each having unique observational characteristics associated with the different dynamic and microphysical processes (e.g., Houze 1993, 1997; Biggerstaff and Houze 1993; Yuter and Houze 1995). This form of precipitation characterization is poorly defined since attempting to uniquely bind a continuous transition from convective to stratiform regions is problematic. There is a belief that existing partitioning methods are still useful toward evaluating several model microphysical behaviors within bulk regions for which a particular physical process dominates (e.g., riming, aggregation) or in the context of other bulk latent heating profiling considerations (e.g., Tao et al. 1990; Schumacher et al. 2004). Reviews of observational partitioning methods in the context of model sensitivity have been previously provided in Lang et al. (2003). Model deficiencies for such efforts make it difficult to determine a preferable method, but it is clear that substantial differences are often observed between solely rainfall-based thresholds and other possible approaches. We present only the ground-based disdrometer component from the ARM Darwin site that was unable to benefit from collocated ARM vertically pointing cloud radar systems having short wavelength and frequent outages that prohibit comparisons with convective–stratiform methods developed using radar profile insights (e.g., so-called brightband stratiform or vertical velocity signatures of convection; Giangrande et al. 2013).

For this study, two convective–stratiform partitioning criteria common to disdrometer-based efforts are considered. One criterion is a basic rainfall-rate threshold of $10\,\mathrm{mm\,h^{-1}}$ [herein called the rainfall-rate criterion (RRC), as in Tokay and Short (1996), Nzeukou et al. (2004), and others]. Such treatments are simple to implement, yet may misclassify convective ''big drop'' or comparable sorting regimes at the periphery of convective lines as well as the edges of convective cells (often adjusted by including periphery assumptions). Initially, we tested a $10\,\mathrm{mm\,h^{-1}}$ cutoff, similar to a basic

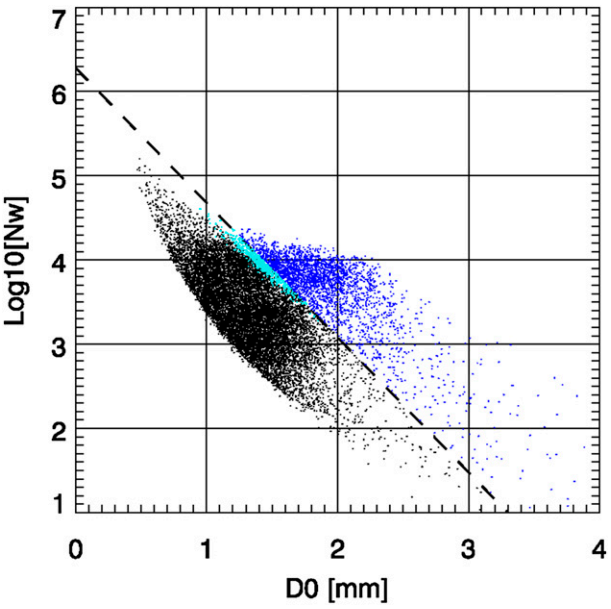

FIG. 4. Scatterplot of disdrometer estimated D_0 and N_w with convective–stratiform segregation line according to Bringi et al. (2009) (dashed). Points that are black are classified as stratiform by the BRC. Dark blue points represent the set adhering to Bringi et al. (2009) convective classifications. Light blue points represent those additional DSDs and associated parameters having rainfall rates $> 10\,\mathrm{mm\,h^{-1}}$, yet still considered stratiform by BRC methods.

Z-based method (e.g., Steiner et al. 1995) that recommends a threshold of 40–42 dBZ according to typical tropical rainfall behavior.

Convective rain, as defined through multimoment DSD definitions for the Darwin tropical precipitation environment, may also demonstrate unique two-dimensional clusters that are well associated with those regimes (e.g., Tokay and Short 1996; Testud et al. 2001; Bringi et al. 2009). The second criterion option for this study follows an empirical formulation utilizing disdrometer measurements of D_0 and N_w as from Bringi et al. (2009):

$$\log_{10}(N_w) = -1.6D_0 + 6.3, \tag{4}$$

where (4) was established at Darwin with additional information from vertical profilers (herein called the Bringi criterion, or BRC). Visual inspection of ARM JWD multiparameter scatterplots hints at similar evidence of two distinct precipitation groupings that are well separated in the N_w–D_0 space. Figure 4 shows a scatterplot of D_0 and $\log_{10}(N_w)$ where points that are classified as convective by the BRC are colored dark blue. Points that are black are classified as stratiform by the BRC. Light blue points are classified as stratiform by the BRC but have rainfall rate $> 10\,\mathrm{mm\,h^{-1}}$ and so are classified as

convective precipitation by the RRC. As from Fig. 4 and cumulative precipitation totals, these two classification methods do not indicate a substantial discrepancy (<5% total accumulation). Here, we have elected to adopt the more stringent convective flag, BRC as in (4), for the remainder of manuscript images when considering convective DSD behaviors, but discuss both behaviors throughout.

2) REGIMES OF THE WET SEASON: WIND AND THERMODYNAMIC PROFILE SEGREGATION

Significant wet season rainfall in Darwin stems from convective modes having distinct forcing and life cycle characteristics that may be reflected back into the observed DSD records. Deeper convection that propagates over Darwin is often continental in origin, whereas shallow convection is more maritime (Drosdowsky 1996; May and Ballinger 2007). Pope et al. (2009) explored the variability of the north Australian wet season according to a cluster analysis on Darwin radiosonde wind and thermodynamic fields. The study considered the 23 UTC soundings over a multidecadal period through 2006 that derived five separate wet season states, unique according to synoptic conditions and rainfall characteristics. Once again, two of the Pope et al. (2009) regimes, a deep west (hereinafter, DW-active) mode and the moist east (hereinafter, ME-break) mode, were shown to be well associated with so-called active shallow convective environments and break–build-up deep convective periods of the monsoon, respectively. Additional regimes, a dry east (DE) regime and east (E) regime, often lacked sufficient moisture at lower levels for significant precipitation development. A final regime, shallow west (SW), is a hybrid monsoonal regime associated with a ''suppressed monsoon'' (May et al. 2008).

To explore connections between monsoonal regimes and DSD variations, we have extended the Pope et al. (2009) clustering methodology to include the 2006–11 wet seasons (see again Fig. 3, red trace). A similar regime segregation was also recently explored for multiyear Darwin polarimetric radar studies as in Kumar et al. (2013) and Penide et al. (2013). Radiosonde launches were performed by the Australian Bureau of Meteorology at the Darwin airport location, in close proximity to the ARM facility (as in Fig. 1). For this study, focus is on the DW-active and ME-break regimes best associated with conventional monsoon active and break convective conditions, respectively. A ''nearest neighbor'' practice around the 2300 UTC radiosonde launch time is employed to project a particular regime classification to a particular DSD observation. One strength of this radiosonde clustering methodology for this task is that the proposed methodology is an objective partitioning to the JWD and rainfall dataset, with Pope et al. (2009) monsoonal modes shown physically significant to traditional monsoonal phases. It is noted that the rainfall-based onset dates as from Table 1 showed strong agreement with the first multiday occurrence of a DW regime.

3) MADDEN–JULIAN OSCILLATION

The role of the MJO on the characteristics of precipitation has been previously discussed (e.g., WH; Lau and Wu 2010) and may influence convective conditions and associated DSD properties during active and inactive phases. The 2006–11 ARM Darwin JWD DSD record has been characterized according to the daily real-time MJO index developed by WH. As with previous monsoonal states, a WH index phase and amplitude was assigned for a particular calendar day (see Fig. 3, green curves). Only those conditions having amplitude values greater than 1 were considered for this study, although allowing larger-scale MJO designations of all amplitudes did not dramatically alter the findings of this study. Active MJO phases are associated with a WH phase value of 4 and 5 for the Darwin location (WH-active). Nonactive phases of the MJO are those having WH phase values of 1 and 8 on the cycle (WH-nonactive).

3. Results

For this study, 14 741 valid DSDs are available at the 5-min aggregation windows (drawn from an archive of 70 000 1-min precipitation DSDs meeting similar quality control standards). As in Table 1, the average wet season during this campaign recorded over 1900 mm, although we report substantial interannual variability connected to several factors previously covered. Since the ARM JWD platform is well suited to estimate rainfall rate R and reflectivity factor Z, a simplified technique to investigate changes in bulk Darwin DSD characteristics associated with larger-scale regimes is through calculation of coefficients associated with standard empirical $R(Z)$ rainfall relations of the form $Z = aR^b$. For comparisons to previous Darwin studies, these calculations are performed using the 1-min DSD records. For the entire ARM dataset, the ''matched'' or reference climatological $R(Z)$ behavior (Rayleigh, matched behavior that reduces the uncertainty in rainfall rate) was found to be $Z = 239R^{1.48}$. As one additional method to align comparisons across various regime behaviors and with previous studies, a similar though less optimal fit can also be performed assuming a fixed b-coefficient exponent, $b = 1.4$. Note that the value of this exponent is comparable to a value associated with the continental rainfall algorithm by the operational Next Generation

TABLE 2. Breakdown of select DSD statistics and parameter calculations segregated according to rainfall-rate interval. Median values are reported and largely correspond with mean values except within low rain rate ($R < 2\,\mathrm{mm\,h^{-1}}$) DSDs having JWD drop sampling issues.

All monsoons median ($\mathrm{mm\,h^{-1}}$)	No. DSD	R ($\mathrm{mm\,h^{-1}}$)	D_0 (mm)	D_m (mm)	Z (dBZ)	W ($\mathrm{g\,m^{-3}}$)	N_0 ($\mathrm{mm^{-1}\,m^{-3}}$)
$0.5 < R < 2$	6149	0.991	1.216	1.270	25.1	0.06	2866
$2 < R < 4$	2806	2.785	1.367	1.437	30.9	0.16	4532
$4 < R < 6$	1349	4.882	1.417	1.491	33.9	0.27	6784
$6 < R < 10$	1170	7.739	1.447	1.521	36.3	0.42	10 010
$10 < R < 20$	1382	13.899	1.573	1.648	39.7	0.74	13 567
$20 < R < 40$	976	27.533	1.815	1.899	44.5	1.40	13 487
$40 < R < 60$	394	48.180	1.970	2.064	47.8	2.38	16 611

Weather Radar (NEXRAD) network (Fulton et al. 1998) and similar to previous Darwin studies including those using JWD disdrometers (e.g., Tokay and Short 1996; Maki et al. 2001). This calculation determined a matched dataset relationship of $Z = 256R^{1.4}$.

Table 2 contains the breakdown of selected DSD and rainfall-rate parameters using a 5-min DSD aggregation window and segregated according to distinct rainfall-rate intervals. On this table, each value represents the median value within the particular rainfall-rate interval and very often corresponds with the associated mean value calculation. This type of nonsequential, median value sampling of DSD parameters as a function of rainfall rate should act to reduce random system (e.g., miscalibration) and some physical process noise (e.g., Lee and Zawadzki 2005; Cao and Zhang 2009); however, this sort of single-dimensional filtering will not completely mitigate all mixing of physical processes in time. Use of the median values rather than mean values should help reduce some uncertainty associated with outlier or poorly sampled DSD, which is problematic at the lower rainfall rates for JWD platforms.

a. Convective–stratiform regime segregation

As listed in Table 1, BRC-classified DSDs indicate that a relatively high fraction [typically ~(62%–70%)] of total rainfall is associated with convective regimes. As one Darwin reference, Tokay and Short (1996) previously reported 68% of total rainfall as convective. The cumulative 5-yr dataset behavior was found to be 67.5%. The lowest fractional convection behavior was observed during the 2010/11 wet season at 62%. During this 2010/11 season, additional uncertainty when performing this BRC separation can be attributed to precipitation collected during the days sampling Tropical Cyclone Carlos and its potential handling under the BRC convective–stratiform classification. Note, if this event was removed from consideration, the convective fraction for the remainder of the 2010/11 season was found to be 64%. As a reminder, if the less-restrictive RRC classification is applied, the average convective fraction increases by 3%.

Figure 5 presents the histograms for several DSD parameters according to an assignment following the BRC convective and stratiform classification. For Fig. 5, we have elected to plot JWD parameters most likely to be well estimated by the JWD platform (Z, W, D_m, and N_0). Joint behaviors for D_0 and W are provided for convective and stratiform regimes in Fig. 6 with associated best-fit curves $W = 0.66D_0^{1.05}$ for convective breakdowns and $W = 0.11D_0^{0.33}$ for stratiform DSDs. On these plots, W is plotted in log scale (dBm units) as in Tokay and Short (1996). Diurnal segregation (the total dataset accumulation stratified according to hour) in following BRC DSD breakdowns is provided in Fig. 7. The reference $R(Z)$ behavior for the entire set of convective DSDs under BRC definitions was determined to be $Z = 86R^{1.74}$. This relationship mapped to $Z = 263R^{1.4}$ if adhering to a fixed b coefficient. The reference "stratiform" $R(Z)$ relationships were determined to be $Z = 230R^{1.59}$ and $Z = 256R^{1.4}$, respectively. It is noteworthy that the convective relations were sensitive to the presence of so-called transitional DSDs wherein RRC and BRC definitions disagree (as in Fig. 4). According to RRC definitions, the convective relations were found as $Z = 55R^{1.85}$ and $Z = 233R^{1.4}$, while stratiform relations were found as $Z = 222R^{1.7}$ and $Z = 261R^{1.4}$, respectively.

b. Monsoonal regime and MJO breakdowns

Table 1 includes the breakdown of Pope et al. (2009) ME-break and DW-active regime fractional precipitation. The ME-break regime was associated with the highest amount of precipitation falling at the Darwin site, having an average wet season accumulation contribution of 700 mm, or an average 37% of the seasonal total. The DW-active monsoon conditions were associated with the second highest contribution to the precipitation (an average wet season of 630 mm attributed to DW-active conditions for Darwin), 33% of the average wet season total. We note that DW-active regime properties include an outlier 2010/11 wet season wherein 54% of the total precipitation was attributed to DW

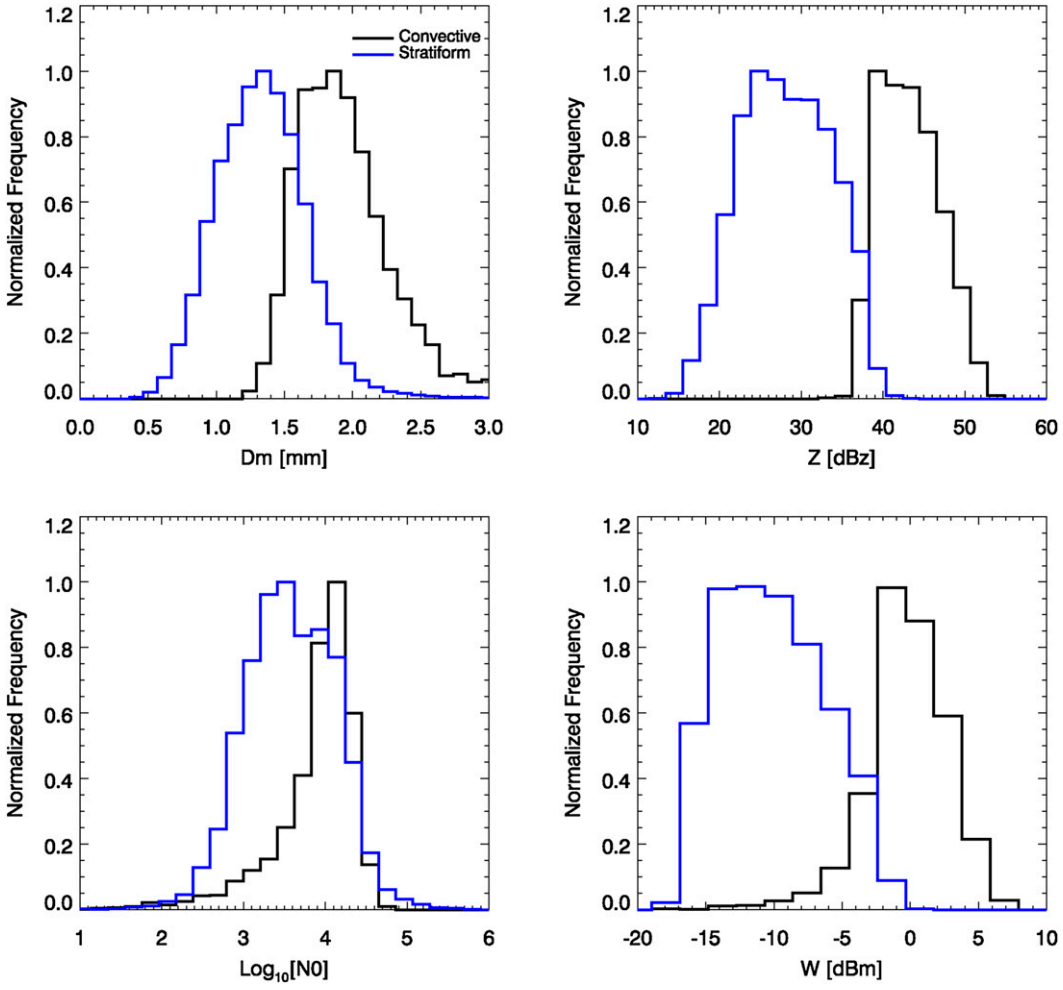

FIG. 5. Histograms of relative distributions of disdrometer measured parameters (top left) D_m, (top right) Z, (bottom left) N_0, and (bottom right) W contingent on Bringi et al. (2009) convective and stratiform segregation results.

regime conditions (including all contributions from the TC Carlos event). It is worth noting that in no other wet season did the relative contribution attributed for the DW-active regime exceed 26%. Although not considered within this study, the additional Pope et al. (2009) SW suppressed monsoonal conditions and E or build up regimes accounted for approximately 21% and 4% of the precipitation in this dataset, respectively.

Figure 8 stratifies the observed DSD parameters according to the ME-break and DW-active regimes. These figure results include a total of 5904 ME-break and 4856 DW-active DSDs. A similar plot is found in Fig. 9, containing only those ME-break and DW-active DSDs classified as convective. This additional convective segregation was included as an approach to further test arguments suggesting ME-break conditions are favorable to deeper land-based convection having vigorous updrafts that support larger drop development (e.g., Bringi et al. 2009; Thurai et al. 2010). Figure 9 monsoonal plots having contingent convective breakdowns include a smaller set of 980 DSDs within ME-break regimes and 872 DSDs in the DW-active regimes. A diurnal plot for DW-active versus ME-break monsoonal accumulations (as in Fig. 7, total accumulation per hour interval) is located in Fig. 10. A check of $R(Z)$ relationships reveals ME-break conditions to be associated with $Z = 247R^{1.49}$, or $Z = 265R^{1.4}$ for a fixed $b = 1.4$. The DW-active conditions were associated with $Z = 217R^{1.47}$, or $Z = 231R^{1.4}$.

Figure 11 contains the partitioning of the ARM JWD dataset parameters according to MJO phase. Recall again that over the Darwin ARM site, the WH-active MJO phase corresponds to an WH index value of 4 and 5, whereas WH-nonactive phases correspond to phase

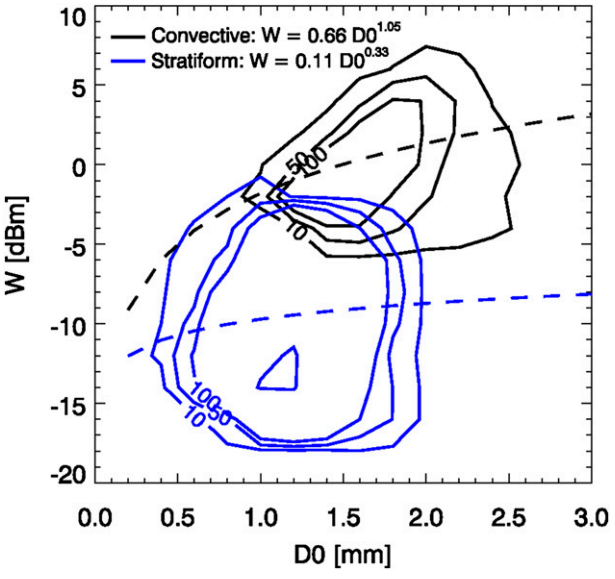

FIG. 6. Joint distribution (counts; contours) of liquid water content W and D_0 for stratiform (black) and convective (blue) DSD segregation from Bringi et al. (2009) methods. Dashed lines represent a best-fit curve for each population.

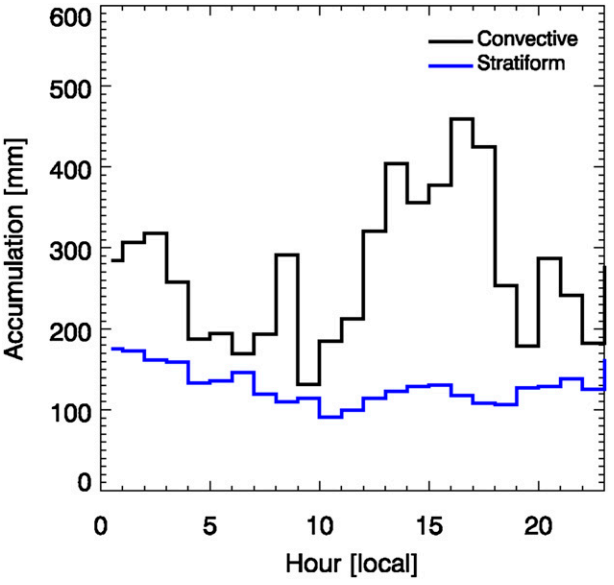

FIG. 7. Diurnal behavior of rainfall over the Darwin ARM location for convective and stratiform DSD segregations according to the Bringi et al. (2009) method.

WH index values of 1 and 8. For these images, 3325 valid DSD samples were obtained under WH-active phases of the MJO, while 1414 DSDs were collected during WH-nonactive MJO phases. Although not included on Table 1, the WH-active MJO phases accounted for approximately twice the precipitation of the WH-nonactive phases for this dataset, or approximately 33% and 17% of the average seasonal totals, respectively. The diurnal breakdown (e.g., Figs. 7, 10) was inconclusive (weak diurnal signature having a minimum accumulation around 1000 UTC and maximum around 1600–1700 UTC) and having no significant difference in relative diurnal variability. The $R(Z)$ relationships as calculated for MJO conditions were found similar for both sets of WH MJO breakdowns, having a relationship of $Z = 240R^{1.46}$. This $R(Z)$ was similar to the climatological reference behavior that included all DSDs collected by the JWD. For a fixed b coefficient, the relationship for these MJO phases was found to be $Z = 254R^{1.4}$.

For additional insight on the potential for cross-coupled regime behaviors, Figs. 12 and 13 include DSD parameter histogram breakdowns for ME-break and DW-active monsoonal conditions contingent on MJO phase. The histogram counts are as follows: ME-break monsoon conditions include 1277 (625) DSDs for WH-active MJO (WH-nonactive MJO), while DW-active monsoon conditions include 1074 (274) DSDs for WH-active MJO (WH-nonactive MJO). For the DW-active monsoon conditions, the reference $R(Z)$ behaviors were calculated as $Z = 25R^{1.51}$ and $Z = 208R^{1.45}$ for WH-nonactive and WH-active MJO phases, respectively. These correspond to $Z = 264R^{1.4}$ and $Z = 219R^{1.4}$ when applying a fixed b-coefficient estimate. Under prevailing ME-break monsoon conditions, the $R(Z)$ relationships according to the MJO phase were calculated as $Z = 261R^{1.44}$ and $Z = 261R^{1.5}$, for WH-nonactive and WH-active MJO phases, respectively. For the fixed b coefficient, these relationships mapped to $Z = 268R^{1.4}$ and $Z = 277R^{1.4}$.

4. Discussion and comparison to other studies

This section compares the depictions of the north Australian wet seasons covered by this study to those depictions found in other studies. Based on Table 1 and Fig. 3, there is basic agreement with previous work including Nicholls et al. (1982, 1984) and Smith et al. (2008) regarding typical Darwin wet season conditions including patterns of onset dates and morphology. The dataset average wet season total (1900 + mm) was found higher than a previous Darwin long-term average (~1650 mm; Smith et al. 2008). However, the JWD dataset average was heavily influenced by the record-setting 2010/11 wet season that saw the ARM Darwin disdrometer site record approximately 2700 mm. Despite the known interannual variability observed for seasonal precipitation, the fractional convective precipitation over Darwin was relatively stable and consistent with

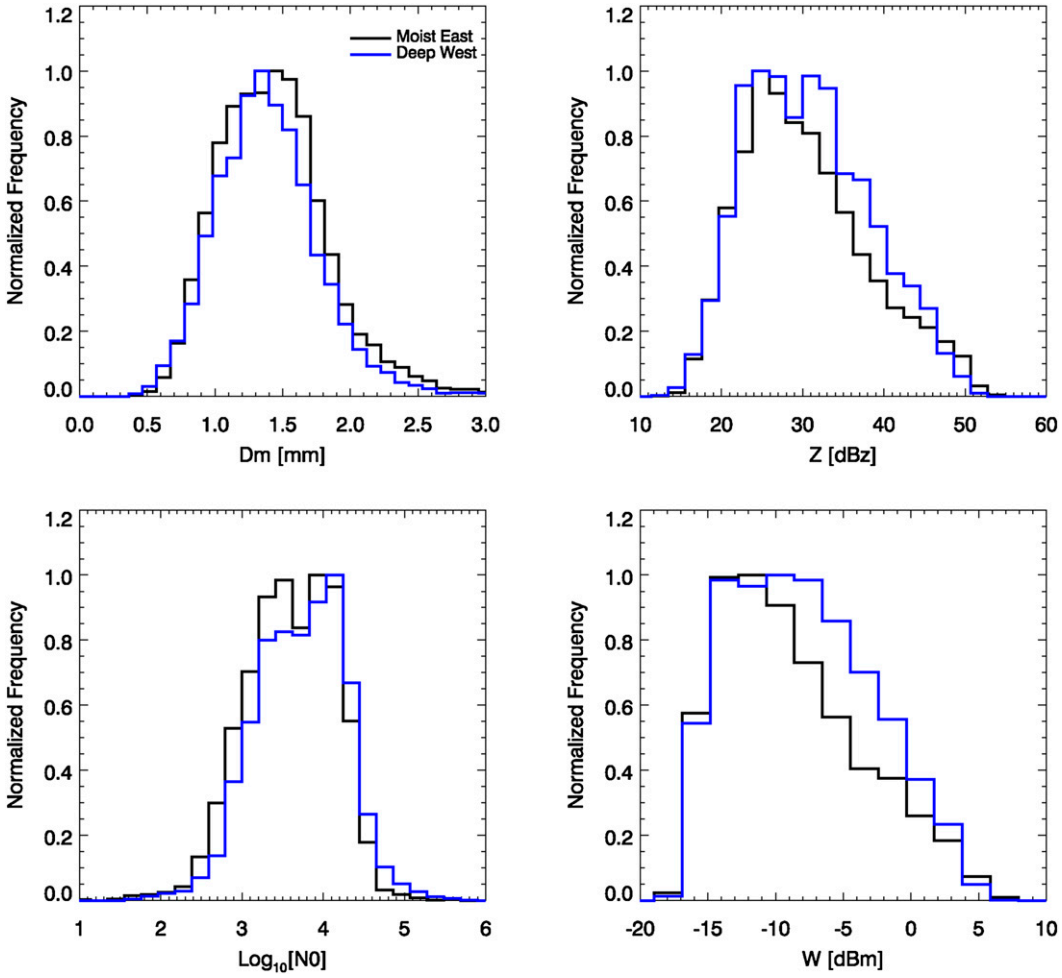

FIG. 8. As in Fig. 5, but for ME-break and DW-active monsoon conditions following Pope et al. (2009).

previous Darwin rainfall studies [~(67%–70%); e.g., Tokay and Short 1996].

As highlighted with Fig. 2, confidence in the ARM disdrometer capture of precipitation was strengthened when considering the solid agreement between the well-maintained, independent ARM surface rainfall platforms (disdrometer and gauges). However, uncertainty attributed to the sampling of precipitation by these platforms was still significant but found to be within 10% of the seasonal rainfall accumulation. Additional uncertainty in seasonal and fractional convective accumulation can be attributed to disdrometer quality control methods to remove low drop count light rain DSDs [~(1%–2%)] of the total accumulation) as well as tropical systems of uncertain DSD behaviors (e.g., TC Carlos). This study also adopts a Bringi et al. (2009) two-moment convective segregation method found to be more restrictive (~3% of the total accumulation) than the standard rainfall-rate threshold (e.g., Fig. 4) having important overlap between stratiform DSD properties in additional (W, Z) or joint (D_0–W) parameter space (e.g., Figs. 5, 6).

The full-dataset $R(Z)$ relation was calculated as $Z = 239R^{1.48}$, or $Z = 256R^{1.4}$ if fixing the exponent b coefficient to $b = 1.4$. This intercept a coefficient $a = 256$ is lower than that utilized by the standard NEXRAD Z–R continental relation having similar exponent $b = 1.4$. These coefficients may be interpreted as Darwin DSD records having higher concentrations of smaller drops than those of continental precipitation. This result is not surprising for tropical precipitation and agrees well with recent Darwin radar-based studies (e.g., Bringi et al. 2009; Thurai et al. 2010; Penide et al. 2013). The estimated $R(Z)$ intercept coefficient is slightly higher than seminal tropical cumulative campaign references (tuned radar-to-gauge; e.g., Steiner et al. 1995; $Z \sim 167R^{1.25}$) or the tropical NEXRAD relationship $Z \sim 230R^{1.25}$ (e.g., Fulton et al. 1998). However, the result falls within the

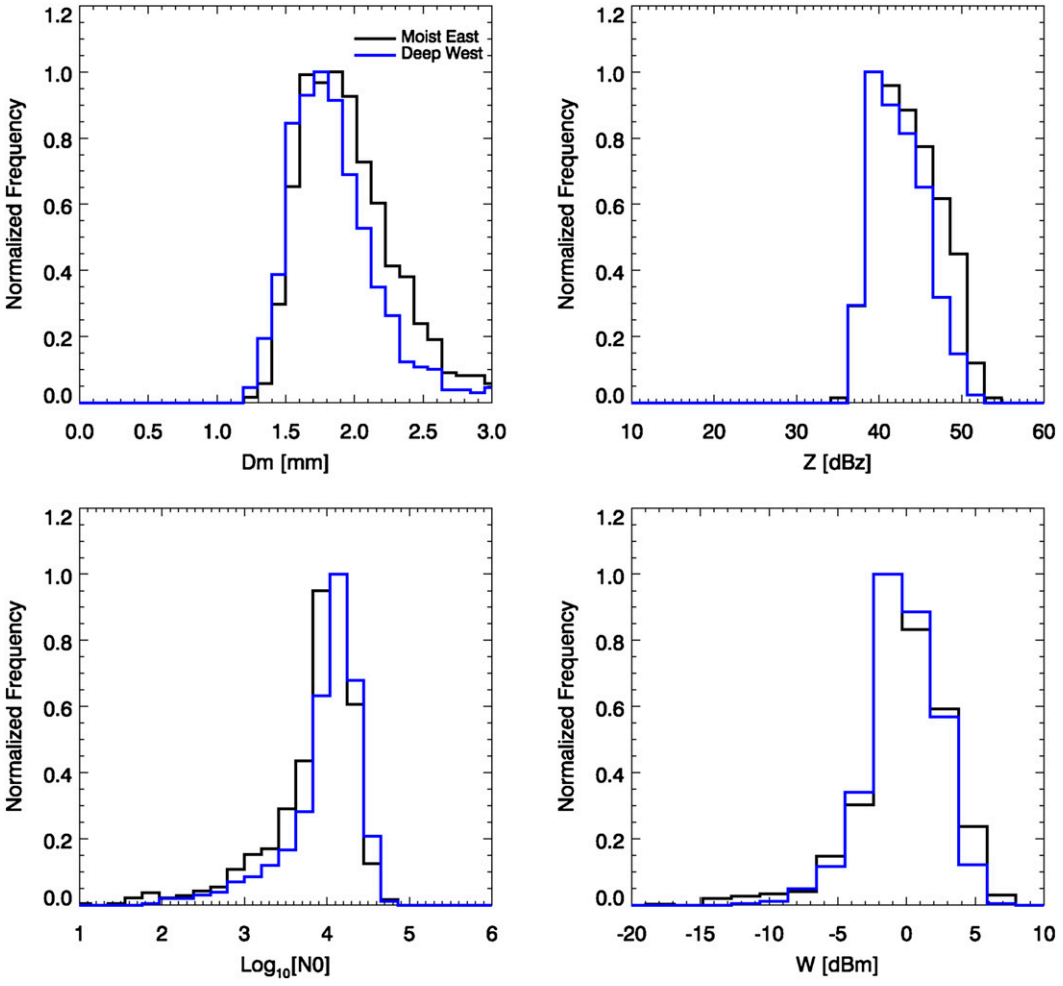

FIG. 9. As in Fig. 8, but for convective DSDs defined by the Bringi et al. (2009) method.

range of previous Darwin JWD studies of Tokay and Short (1996; $Z \sim 315R^{1.2}$) and Maki et al. (2001; $Z \sim 232R^{1.38}$).

One possible explanation for higher relative a coefficients may be reflected in the values of the ARM JWD median bulk drop size (e.g., Fig. 5, Table 2) as compared to histograms and rainfall-based DSD properties found in previous studies (e.g., Bringi et al. 2009; Thurai et al. 2010; Penide et al. 2013). A known limitation of the JWD disdrometer system is sampling smaller drop sizes and this necessitates a standard dead-time correction that may not be adequate within a challenging tropical environment. A persistent absence of smaller drops is consistent with higher intercept values since smaller drops less influence the estimate of Z than the rainfall rate R. Nevertheless, modest $R(Z)$ coefficient inconsistencies are unavoidable if comparing across the results of many isolated Darwin campaigns that have selectively sampled from particular subsets of stronger convective storm populations [having lower-relative intercept a coefficient; e.g., as in squall line events from Maki et al. (2001)].

The most prominent bulk regime signal observed within this study was that associated with the diurnal cycle for convective–stratiform and monsoonal conditions. Regime segregation for convective DSDs and those DSDs from ME-break conditions (e.g., Figs. 7, 10) demonstrate preferential rainfall accumulation within the afternoon hours over Darwin. This is consistent with previous studies (e.g., Kumar et al. 2013) that there is an expectation for land-based deep convective cells at Darwin during the monsoon break period having a similar afternoon onset time. A secondary precipitation peak in the early morning was observed, although it was more pronounced for the convective regime than the ME-break regime. The agreement between Darwin diurnal signatures as recorded by the JWD, as well as the increased magnitude of precipitation observed during

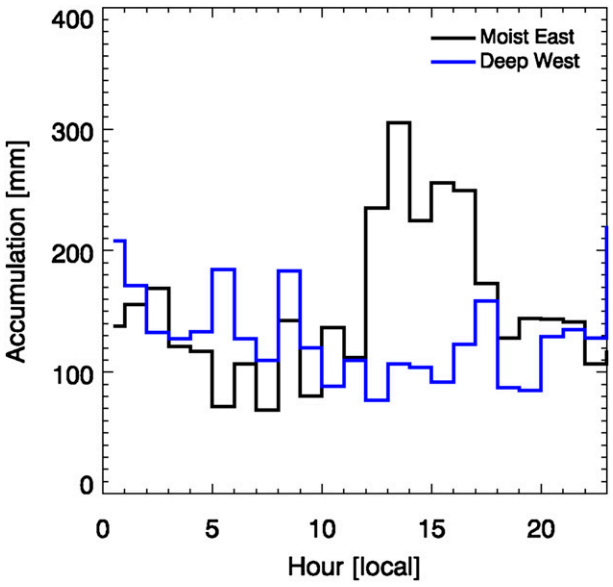

FIG. 10. As in Fig. 7, but for ME-break and DW-active monsoon conditions following Pope et al. (2009).

the typical wet season under ME-break regimes (e.g., Table 1), supports the Kumar et al. (2013) suggestion for the ME-break regime as a default climatology of Darwin. In contrast, the stratiform regime and the DW-active monsoonal condition demonstrate no preferential precipitation cycle at Darwin other than a faint diurnal signature, also in keeping with Kumar et al. (2013) findings.

The DSD parameter breakdowns listed in Table 2 and further illustrated for regime breakdowns within Figs. 5, 6, 8, and 9 match well with the findings of previous Darwin convective–stratiform and/or monsoonal rainfall studies over land (e.g., Bringi et al. 2009; Thurai et al. 2010; Penide et al. 2013). This study helps strengthen previous arguments from those efforts that suggest that ME-break condition (as plotted in histograms) favors larger drop sizes, higher Z extremes, and narrower distributions for W fields. In particular, we find solid qualitative agreement with the joint DSD parameter observations for land-based convection as in Thurai et al. (2010) that suggest ME-break (DW-active) conditions exhibit smaller (larger) number concentrations associated with larger (smaller) drop sizes (e.g., Figs. 8, 9). It follows that these relative larger drop DSD characteristics are also consistent with an ME-break condition that featured larger relative intercept a coefficients for $R(Z)$ rainfall relations ($a = 248$ and 265) than that for the DW-active periods ($a = 217$ and 231) for similar exponents ($b = 1.48$ and 1.4).

Similarly, bulk convective conditions favored higher number concentration, D_m, Z, W, and joint D_0–W distributions (e.g., Figs. 5, 6). This was reflected in comparable or smaller intercept a coefficient for convection as compared to the stratiform regime DSDs. The separations were pronounced when considering convection contingent on monsoonal region, for example, convection within DW-active conditions favoring higher concentrations of smaller drops (Fig. 9). The relative behaviors are consistent with previous Darwin and tropical precipitation efforts (e.g., Steiner et al. 1995; Tokay and Short 1996; Cifelli et al. 2000; Maki et al. 2001; Thurai et al. 2010). We determine an intercept coefficient of $a = 233$ for this ARM disdrometer dataset when stratified according to the RRC segregation procedure using a fixed exponent $b = 1.4$ (for stratiform, $a = 261$). Using a similar procedure, convective and stratiform intercept parameters were found nearly identical under the BRC segregation ($a \sim 260$). In the case of RRC (BRC) segregations, the observed intercept coefficient for convection is consistent (higher) with the values reported in several tropical convective studies having similar convective definitions of b-coefficient magnitudes (e.g., Steiner et al. 1995; Tokay and Short 1996; Maki et al. 2001). However, it is misleading to attribute too much insight to these fixed exponent results, as the optimal relations obtained when fitting both the intercept and exponent parameters simultaneously indicate both BRC and RRC sets of convective relations predict substantially smaller Z relative to similar R (e.g., smaller bulk drop sizes). In this way, the ARM disdrometer findings still support similar findings for convective populations as compared with stratiform populations. It is not surprising that these results are in closest alignment with the intercept and exponent values fitted in previous campaigns employing a JWD platform for Darwin (e.g., Tokay and Short 1996; Maki et al. 2001). Less agreement was observed when comparing the coefficients to the tropical and/or Darwin $R(Z)$ relationships obtained from radar–rain gauge studies (e.g., Steiner et al. 1995) or when using wind profiler system retrievals (e.g., Cifelli et al. 2000). This disagreement with radar-driven studies may be anticipated according to differences in instrument sampling volumes and spatial-temporal geometrical matching considerations.

Note again that the handling of transitional DSDs having parameters that fall under one convective definition RRC, but not the other BRC, was an important consideration and possible ''contaminant'' if comparing convective coefficients to previous studies (e.g., Uijlenhoet et al. 2003). This can be especially problematic since identifying the transition region is not a well-posed problem. These regions have been previously shown to feature modest ranges of rainfall rates associated with an absence of larger drop sizes linked back to lower

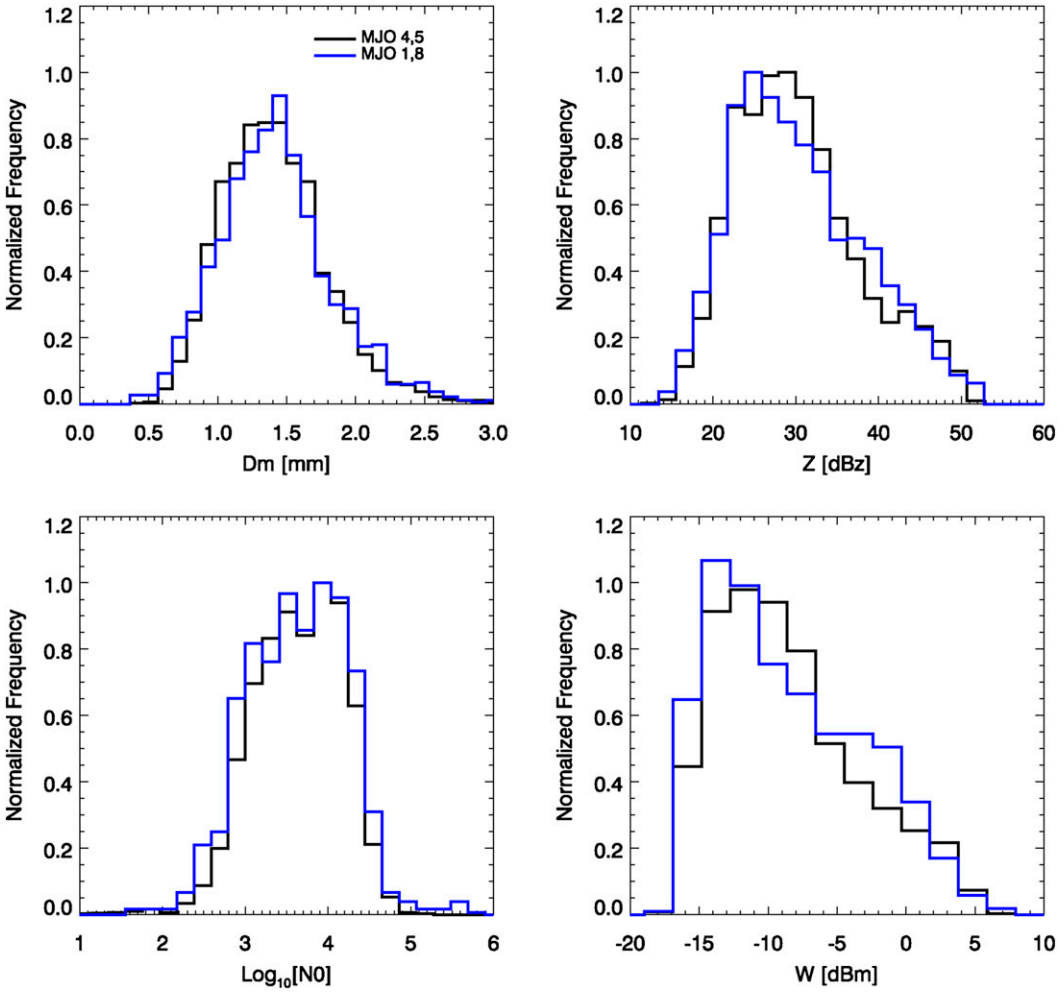

FIG. 11. As in Fig. 5, but segregated according to WH MJO phase (4,5–active over Darwin; 1,8–nonactive over Darwin) having amplitude > 1.

intercept coefficients (e.g., Houze 1993; Biggerstaff and Houze 1993; Schuur et al. 2001; Uijlenhoet et al. 2003; Giangrande et al. 2012). Although the choice of convective segregation was not significant to the total convective fraction (within 3%), the RRC method allows additional smaller drop DSDs recording a modest rainfall rate $R > 10\,\mathrm{mm\,h^{-1}}$ (RRC definition) having coupled low median drop size and/or number counts (e.g., Fig. 4). Note that coefficient sensitivity was less of a concern for stratiform relations owing to a larger number of samples (stratiform DSDs outnumbered convective DSDs by a factor of 5). For convective classifications, including this set of transitional DSDs in the RRC relations reduced the apparent intercept a coefficient from 260 (BRC) to 230 (RRC) if adhering to a fixed exponent $b = 1.4$. However, although these transitional DSDs also influenced the results of joint exponent–intercept parameter fits, here the convective relations under both BRC and RRC definitions suggest substantially lower intercepts and higher exponents than stratiform counterparts (e.g., Tokay and Short 1996).

When ARM dataset results are stratified according to cumulative MJO influences for the Darwin location, the results were found to be inconclusive or nonexistent. WH-active MJO phase conditions over Darwin were on average associated with twice the rainfall accumulation of the WH-nonactive MJO phases. Unlike previous convective or monsoonal regime modes, we observe no diurnal signature separation between WH-active and WH-nonactive MJO phases over Darwin. Rainfall parameter calculations for the intercept and exponent coefficients in the $R(Z)$ relations suggest no clear separation between the WH MJO modes. Here, it was found that both WH phases shared similar $R(Z)$ coefficients with the all-dataset climatological relationship, having an a coefficient close to 250 when the intercept was fixed

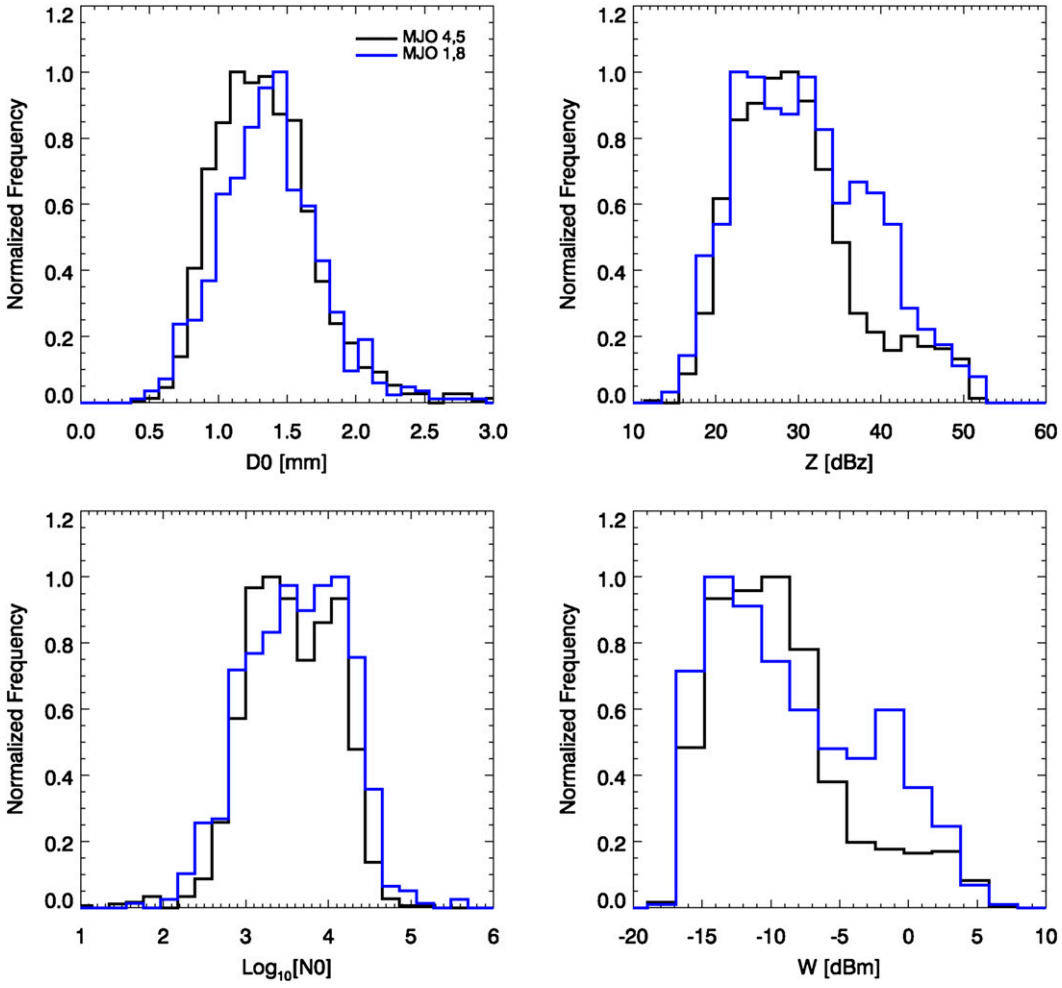

FIG. 12. MJO phase breakdowns as in Fig. 11, but for ME-break conditions.

as $b = 1.4$. Histograms in Fig. 11 also illustrate this lack of a significant separation between the MJO WH-active and WH-nonactive populations. The application of a standard statistical test (e.g., *t* test, Mann–Whitney) is arguably not well posed for precipitation datasets of this sort, having measured DSDs that are not likely independent from one to the next. However, when such testing was applied to MJO phase conditions found in this study, WH-active versus WH-nonactive MJO populations were the only subset of regimes that registered the likelihood of similar DSD populations.

As comment toward future efforts, the ARM dataset is still limited in reference to possible DSD behaviors associated with the coupling of MJO phase to monsoonal larger-scale regimes (e.g., Figs. 12, 13). As a preliminary effort, the ARM dataset highlights a possibility that DW-active monsoon phases coupled with WH-active MJO phases tended toward the more unique behaviors, a pronounced monsoonal or tropical condition sampled at Darwin (e.g., exhibiting higher relative drop concentrations and Z and W histogram behaviors as compared to WH-nonactive MJO phases). This regime cross coupling may be best viewed in relative $R(Z)$ behaviors wherein the DW-active regime and WH-active MJO coupling was associated to a very low a coefficient ($a = 219$, for fixed b coefficient) linked with higher counts of smaller drops. This particular DSD subset was limited, but the behaviors were not influenced by an extreme tropical cyclone event such as TC Carlos or TC Helen. Remaining couplings of monsoon and MJO phases demonstrate similar behavior in terms of relative a coefficients ($a \sim 265$–277). A complementary pairing was also found for the DW-active monsoon conditions coupled with WH-nonactive MJO phases that exhibited similar histogram extremes to the WH-active MJO phase periods under ME-break conditions. Obtaining a better understanding of such coupled behaviors may be better suited for longer-term polarimetric radar

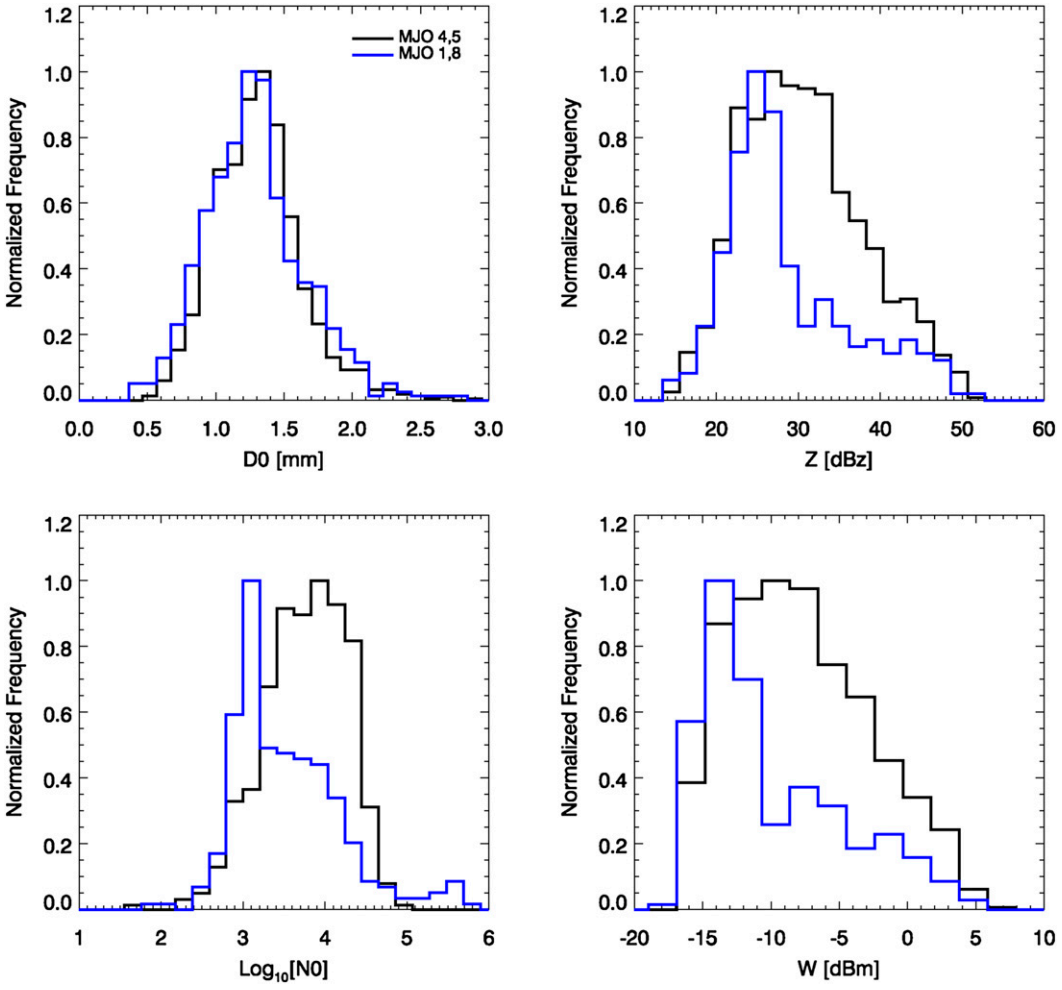

FIG. 13. MJO phase breakdowns as in Fig. 11, but for DW-active conditions.

datasets offering substantially more column or spatial storm properties for Darwin systems (e.g., Kumar et al. 2013; Penide et al. 2013).

5. Summary

The variability of rainfall and select DSD properties as a function of atmospheric conditions and storm characteristics has been summarized for a multiyear disdrometer archive obtained from the ARM facility at Darwin, Australia. Although disdrometer platforms of this sort may have their limitations, the strength of these JWD measurements is in their durability for longer-term deployments to tease out bulk regime behaviors. While the Darwin location may not be the optimal placement for northern Australia studies on ME-break and DW-active phases because of the site placement (according to the timing and nature of propagating convection over land that reaches this facility), there is still considerable sampling of events to consider the insights provided as support for climate modeling improvement efforts. The key findings of this study are as follows:

1) Darwin cumulative and seasonal wet season depictions matched those found in previous campaign efforts including records for average seasonal precipitation (1900 mm), monsoon onset date (mid- to late December), fractional convective precipitation (67%), and diurnal signatures. DSD parameter distributions strengthen previous arguments for land-based systems around Darwin indicative of high concentrations of smaller drops (e.g., Tokay and Short 1996; Thurai et al. 2010; Kumar et al. 2013; Penide et al. 2013). Associated $R(Z)$ relationships for convective storms ($Z = 233R^{1.4}$; $Z = 260R^{1.4}$) and the cumulative dataset ($Z = 250R^{1.4}$) are found having low intercept a coefficients compared to continental relations, similar to previous Darwin studies matching radar and/or gauge platforms. Comparisons were also

favorable with the convective–stratiform properties and relations reported in previous Darwin JWD-driven studies.

2) DSD characteristics contingent on monsoonal regime suggest larger drop sizes associated with ME or break monsoon regimes. These findings are consistent with previous Darwin radar studies for land-based cells (e.g., Bringi et al. 2009; Thurai et al. 2010). Larger-drop behaviors are also highlighted for this JWD datasets in the terms of larger relative intercept a coefficients for matched $R(Z)$ relations calculated during ME-break conditions ($Z = 265R^{1.4}$) as compared with DW-active conditions ($Z = 231R^{1.4}$). As with convection, ME-break precipitation exhibits a distinct diurnal maximum in precipitation (~1600 UTC) attributed to afternoon sea-breeze convection (e.g., Fig. 10). This ME-break regime accounts for the most precipitation of any monsoonal regime (37%) during this 5-yr window. The findings are consistent with the Kumar et al. (2013) study that suggests the ME-break regime as a default climatological condition for Darwin.
3) The separation of DSD and rainfall parameters according to MJO phase over Darwin did not illuminate significant diurnal or drop-size behaviors. WH-active MJO phases were responsible for twice the precipitation of nonactive phases. Both WH-active and WH-nonactive phases exhibit limited diurnal characteristics and feature similar matched $R(Z)$ relations close to the climatological behavior (e.g., $Z = 250R^{1.4}$). A coupled active–active phasing of the MJO and monsoon does reveal the most pronounced tropical precipitation behavior for this dataset ($Z = 219R^{1.4}$) and is of interest for future study.

Acknowledgments. This manuscript has been authored by employees of Brookhaven Science Associates, LLC, under Contract DE-AC02-98CH10886 with the U.S. Department of Energy. The publisher by accepting the manuscript for publication acknowledges that the U.S. government retains a nonexclusive, paid-up, irrevocable, worldwide license to publish or reproduce the published form of this manuscript, or allow others to do so, for U.S. government purposes. The efforts of Scott Giangrande were partially supported by the Climate Science for a Sustainable Energy Future project of the Earth System Modeling program in DOE's Office of Science. Argonne National Laboratory's (ANL) work was supported by the U.S. Department of Energy, Office of Science, Office of Biological and Environmental Research, under Contract DE-AC02-06CH11357. In addition, the authors thank the ARM Climate Research Facility for the extended disdrometer dataset (instrument mentor is author Mary Jane Bartholomew) collection and maintenance. We also thank Dr. Yan Feng of ANL for internal review of this manuscript.

REFERENCES

Ackerman, T. P., and G. M. Stokes, 2003: The Atmospheric Radiation Measurement Program. *Phys. Today,* **56,** 38–44, doi:10.1063/1.1554135.

Atlas, D., C. W. Ulbrich, F. D. Marks Jr., E. Amitai, and C. R. Williams, 1999: Systematic variation of drop size and radar-rainfall relations. *J. Geophys. Res.,* **104** (D6), 6155–6169, doi:10.1029/1998JD200098.

Biggerstaff, M. I., and R. A. Houze, 1993: Kinematics and microphysics of the transition zone of the 10–11 June 1985 squall line. *J. Atmos. Sci.,* **50,** 3091–3110, doi:10.1175/1520-0469(1993)050<3091:KAMOTT>2.0.CO;2.

Blossey, P. N., C. S. Bretherton, J. Cetrone, and M. Kharoutdinov, 2007: Cloud-resolving model simulations of KWAJEX: Model sensitivities and comparisons with satellite and radar observations. *J. Atmos. Sci.,* **64,** 1488–1508, doi:10.1175/JAS3982.1.

Bringi, V. N., G. Huang, V. Chandrasekar, and E. Gorgucci, 2002: A methodology for estimating the parameters of a gamma raindrop size distribution model from polarimetric radar data: Application to a squall-line event from the TRMM/Brazil campaign. *J. Atmos. Oceanic Technol.,* **19,** 633–645, doi:10.1175/1520-0426(2002)019<0633:AMFETP>2.0.CO;2.

——, V. Chandrasekar, J. Hubbert, E. Gorgucci, W. L. Randeu, and M. Schoenhuber, 2003: Raindrop size distribution in different climatic regimes from disdrometer and dual-polarized radar analysis. *J. Atmos. Sci.,* **60,** 354–365, doi:10.1175/1520-0469(2003)060<0354:RSDIDC>2.0.CO;2.

——, C. R. Williams, M. Thurai, and P. T. May, 2009: Using dual-polarized radar and dual-frequency profiler for DSD characterization: A case study from Darwin, Australia. *J. Atmos. Oceanic Technol.,* **26,** 2107–2122, doi:10.1175/2009JTECHA1258.1.

Cao, Q., and G. Zhang, 2009: Errors in estimating raindrop size distribution parameters employing disdrometer and simulated raindrop spectra. *J. Appl. Meteor. Climatol.,* **48,** 406–425, doi:10.1175/2008JAMC2026.1.

Cifelli, R., C. R. Williams, D. K. Rajopadhyaya, S. K. Avery, K. S. Gage, P. T. May, 2000: Drop-size distribution characteristics in tropical mesoscale convective systems. *J. Appl. Meteor.,* **39,** 760–777, doi:10.1175/1520-0450(2000)039<0760:DSDCIT>2.0.CO;2.

Dare, R. A., N. E. Davidson, and J. L. McBride, 2012: Tropical cyclone contribution to rainfall over Australia. *Mon. Wea. Rev.,* **140,** 3606–3619, doi:10.1175/MWR-D-11-00340.1.

Del Genio, A. D., 2012: Representing the sensitivity of convective cloud systems to tropospheric humidity in general circulation models. *Surv. Geophys.,* **33,** 637–656, doi:10.1007/s10712-011-9148-9.

Dolan, B., S. A. Rutledge, S. Lim, V. Chandrasekar, and M. Thurai, 2013: A robust C-band hydrometeor identification algorithm and application to a long-term polarimetric radar data set. *J. Appl. Meteor. Climatol.,* **52,** 2162–2186, doi:10.1175/JAMC-D-12-0275.1.

Drosdowsky, W., 1996: Variability of the Australian summer monsoon at Darwin: 1957–1992. *J. Climate,* **9,** 85–96, doi:10.1175/1520-0442(1996)009<0085:VOTASM>2.0.CO;2.

Duchon, C. E., and G. R. Essenberg, 2001: Comparative rainfall observations from pit and aboveground rain gauges with and without wind shields. *Water Resour. Res.,* **37,** 3253–3263, doi:10.1029/2001WR000541.

Fulton, R. A., J. P. Breidenbach, D.-J. Seo, D. A. Miller, and T. O'Bannon, 1998: The WSR-88D rainfall algorithm. *Wea. Forecasting,* **13,** 377–395, doi:10.1175/1520-0434(1998)013<0377:TWRA>2.0.CO;2.

Giangrande, S. E., E. P. Luke, and P. Kollias, 2012: Characterization of vertical velocity and drop size distribution parameters in widespread precipitation at ARM facilities. *J. Appl. Meteor. Climatol.,* **51,** 380–391, doi:10.1175/JAMC-D-10-05000.1.

——, S. Collis, J. Straka, A. Protat, C. Williams, and S. Krueger, 2013: A summary of convective-core vertical velocity properties using ARM UHF wind profilers in Oklahoma. *J. Appl. Meteor. Climatol.,* **52,** 2278–2295, doi:10.1175/JAMC-D-12-0185.1.

Gunn, R., and G. D. Kinzer, 1949: The terminal velocity of fall for water droplets in stagnant air. *J. Meteor.,* **6,** 243–248, doi:10.1175/1520-0469(1949)006<0243:TTVOFF>2.0.CO;2.

Habib, E., W. F. Krajewski, and A. Kruger, 2001: Sampling errors of tipping-bucket rain gauge measurements. *J. Hydrol. Eng.,* **6,** 159–166, doi:10.1061/(ASCE)1084-0699(2001)6:2(159).

Holland, G. J., 1986: Interannual variability of the Australian summer monsoon at Darwin: 1952–82. *Mon. Wea. Rev.,* **114,** 594–604, doi:10.1175/1520-0493(1986)114<0594:IVOTAS>2.0.CO;2.

——, J. L. McBride, R. K. Smith, D. Jasper, and T. D. Keenan, 1986: The BMRC Australian Monsoon Experiment: AMEX. *Bull. Amer. Meteor. Soc.,* **67,** 1466–1472, doi:10.1175/1520-0477(1986)067<1466:TBAMEA>2.0.CO;2.

Houze, R. A., Jr., 1993: *Cloud Dynamics.* Academic Press, 573 pp.

——, 1997: Stratiform precipitation in regions of convection: A meteorological paradox? *Bull. Amer. Meteor. Soc.,* **78,** 2179–2196, doi:10.1175/1520-0477(1997)078<2179:SPIROC>2.0.CO;2.

Jakob, C., 2010: Accelerating progress in global atmospheric model development through improved parameterizations: Challenges, opportunities, and strategies. *Bull. Amer. Meteor. Soc.,* **91,** 869–875, doi:10.1175/2009BAMS2898.1.

Joss, J., and A. Waldvogel, 1967: A raindrop spectrograph with automatic analysis. *Pure Appl. Geophys.,* **68,** 240–246, doi:10.1007/BF00874898.

Keenan, T. D., and R. E. Carbone, 1992: A preliminary morphology of precipitation systems in tropical northern Australia. *Quart. J. Roy. Meteor. Soc.,* **118,** 283–326, doi:10.1002/qj.49711850406.

——, J. McBride, G. Holland, N. Davidson, and B. Gunn, 1989: Diurnal variations during the Australian Monsoon Experiment (AMEX) Phase II. *Mon. Wea. Rev.,* **117,** 2535–2553, doi:10.1175/1520-0493(1989)117<2535:DVDTAM>2.0.CO;2.

——, and Coauthors, 2000: The Maritime Continent Thunderstorm Experiment (MCTEX): Overview and some results. *Bull. Amer. Meteor. Soc.,* **81,** 2433–2455, doi:10.1175/1520-0477(2000)081<2433:TMCTEM>2.3.CO;2.

Kozu, T., T. Shimomai, Z. Akramin, Marzuki, Y. Shibagaki, and H. Hashiguchi, 2005: Intraseasonal variation of raindrop size distribution at Koto Tabang, West Sumatra, Indonesia. *Geophys. Res. Lett.,* **32,** L07803, doi:10.1029/2004GL022340.

Kumar, V. V., A. Protat, P. T. May, C. Jakob, G. Penide, S. Kumar, and L. Davies, 2013: On the effects of large-scale environment and surface types on convective cloud characteristics over Darwin, Australia. *Mon. Wea. Rev.,* **141,** 1358–1374, doi:10.1175/MWR-D-12-00160.1.

Lang, S., W.-K. Tao, J. Simpson, and B. Ferrier, 2003: Modeling of convective–stratiform precipitation processes: Sensitivity to partitioning methods. *J. Appl. Meteor.,* **42,** 505–527, doi:10.1175/1520-0450(2003)042<0505:MOCSPP>2.0.CO;2.

Lau, K.-M., and H.-T. Wu, 2010: Characteristics of precipitation, cloud, and latent heating associated with the Madden–Julian oscillation. *J. Climate,* **23,** 504–518, doi:10.1175/2009JCLI2920.1.

——, and Coauthors, 2000: Report of the field operations and early results of the South China Sea Monsoon Experiment (SCSMEX). *Bull. Amer. Meteor. Soc.,* **81,** 1261–1270, doi:10.1175/1520-0477(2000)081<1261:AROTFO>2.3.CO;2.

Lee, G. W., and I. Zawadzki, 2005: Variability of drop size distributions: Noise and noise filtering in disdrometric data. *J. Appl. Meteor.,* **44,** 634–652, doi:10.1175/JAM2222.1.

Leinonen, J., D. Moisseev, M. Leskinen, and W. A. Petersen, 2012: A climatology of disdrometer measurements of rainfall in Finland over five years with implications for global radar observations. *J. Appl. Meteor. Climatol.,* **51,** 392–404, doi:10.1175/JAMC-D-11-056.1.

Long, C. N., and Coauthors, 2013: ARM research in the equatorial western Pacific: A decade and counting. *Bull. Amer. Meteor. Soc.,* **94,** 695–708, doi:10.1175/BAMS-D-11-00137.1.

Maki, M., T. D. Keenan, Y. Sasaki, and K. Nakamura, 2001: Characteristics of the raindrop size distribution in tropical continental squall lines observed in Darwin, Australia. *J. Appl. Meteor.,* **40,** 1393–1412, doi:10.1175/1520-0450(2001)040<1393:COTRSD>2.0.CO;2.

Marzuki, M., W. L. Randeu, M. Schoenhuber, V. N. Bringi, T. Kozu, and T. Shimomai, 2010: Raindrop size distribution parameters of disdrometer data with different bin sizes. *IEEE Trans. Geosci. Remote Sens.,* **48,** 3075–3080, doi:10.1109/TGRS.2010.2043955.

Mather, J. H., and J. W. Voyles, 2013: The ARM Climate Research Facility: A review of structure and capabilities. *Bull. Amer. Meteor. Soc.,* **94,** 377–392, doi:10.1175/BAMS-D-11-00218.1.

——, T. P. Ackerman, W. E. Clements, F. J. Barnes, M. D. Ivey, L. D. Hatfield, and R. M. Reynolds, 1998: An atmospheric radiation and cloud station in the tropical western Pacific. *Bull. Amer. Meteor. Soc.,* **79,** 627–642, doi:10.1175/1520-0477(1998)079<0627:AARACS>2.0.CO;2.

May, P. T., and A. Ballinger, 2007: The statistical characteristics of convective cells in a monsoon regime (Darwin, Northern Australia). *Mon. Wea. Rev.,* **135,** 82–92, doi:10.1175/MWR3273.1.

——, J. H. Mather, G. Vaughan, K. N. Bower, C. Jakob, G. M. McFarquhar, and G. G. Mace, 2008: The Tropical Warm Pool International Cloud Experiment. *Bull. Amer. Meteor. Soc.,* **89,** 629–645, doi:10.1175/BAMS-89-5-629.

Milbrandt, J. A., and M. K. Yau, 2005: A multimoment bulk microphysics parameterization. Part I: Analysis of the role of the spectral shape parameter. *J. Atmos. Sci.,* **62,** 3051–3064, doi:10.1175/JAS3534.1.

Nešpor, V., and B. Sevruk, 1999: Estimation of wind-induced error of rainfall gauge measurements using a numerical simulation. *J. Atmos. Oceanic Technol.,* **16,** 450–464, doi:10.1175/1520-0426(1999)016<0450:EOWIEO>2.0.CO;2.

Nicholls, N., 1984: A system for predicting the onset of the north Australian wet-season. *Int. J. Climatol.,* **4,** 425–435, doi:10.1002/joc.3370040407.

——, J. L. McBride, and R. J. Ormerod, 1982: On predicting the onset of the Australian wet season at Darwin. *Mon. Wea.*

Rev., **110,** 14–17, doi:10.1175/1520-0493(1982)110<0014:OPTOOT>2.0.CO;2.

Nzeukou, A., H. Sauvageot, A. D. Ochou, and M. F. K. Cheikh, 2004: Raindrop size distribution and radar parameters at Cape Verde. *J. Appl. Meteor.,* **43,** 90–105, doi:10.1175/1520-0450(2004)043<0090:RSDARP>2.0.CO;2.

Penide, G., V. V. Kumar, A. Protat, and P. T. May, 2013: Statistics of drop size distribution parameters and rain rates for stratiform and convective precipitation during the north Australian wet season. *Mon. Wea. Rev.,* **141,** 3222–3237, doi:10.1175/MWR-D-12-00262.1.

Pope, M., C. Jakob, and M. J. Reeder, 2009: Regimes of the north Australian wet season. *J. Climate,* **22,** 6699–6715, doi:10.1175/2009JCLI3057.1.

Rosenfeld, D., D. Wolff, and D. Atlas, 1993: General probability-matched relations between radar reflectivity and rain rate. *J. Appl. Meteor.,* **32,** 50–72, doi:10.1175/1520-0450(1993)032<0050:GPMRBR>2.0.CO;2.

Schumacher, C., R. A. Houze, and I. Kraucunas, 2004: The tropical dynamical response to latent heating estimates derived from the TRMM precipitation radar. *J. Atmos. Sci.,* **61,** 1341–1358, doi:10.1175/1520-0469(2004)061<1341:TTDRTL>2.0.CO;2.

Schuur, T. J., A. V. Ryzhkov, D. S. Zrnić, and M. Schönhuber, 2001: Drop size distributions measured by a 2D video disdrometer: Comparison with dual-polarization radar data. *J. Appl. Meteor.,* **40,** 1019–1034, doi:10.1175/1520-0450(2001)040<1019:DSDMBA>2.0.CO;2.

Sheppard, B. E., and P. I. Joe, 1994: Comparison of raindrop size distribution measurements by a Joss–Waldvogel disdrometer, a PMS 2DG spectrometer, and a POSS Doppler radar. *J. Atmos. Oceanic Technol.,* **11,** 874–887, doi:10.1175/1520-0426(1994)011<0874:CORSDM>2.0.CO;2.

Smith, I. N., L. Wilson, and R. Suppiah, 2008: Characteristics of the northern Australian rainy season. *J. Climate,* **21,** 4298–4311, doi:10.1175/2008JCLI2109.1.

Smith, P. L., D. V. Kliche, and R. W. Johnson, 2009: The bias and error in moment estimators for parameters of drop size distribution functions: Sampling from gamma distributions. *J. Appl. Meteor. Climatol.,* **48,** 2118–2126, doi:10.1175/2009JAMC2114.1.

Steiner, M., R. A. Houze, and S. E. Yuter, 1995: Climatological characterization of three-dimensional storm structure from operational radar and rain gauge data. *J. Appl. Meteor.,* **34,** 1978–2007, doi:10.1175/1520-0450(1995)034<1978:CCOTDS>2.0.CO;2.

Stephens, G. L., 2005: Cloud feedbacks in the climate system: A critical review. *J. Climate,* **18,** 237–273, doi:10.1175/JCLI-3243.1.

Stokes, G. M., and S. E. Schwartz, 1994: The Atmospheric Radiation Measurement (ARM) Program: Programmatic background and design of the Cloud and Radiation Test Bed. *Bull. Amer. Meteor. Soc.,* **75,** 1201–1221, doi:10.1175/1520-0477(1994)075<1201:TARMPP>2.0.CO;2.

Tao, W.-K., J. Simpson, S. Lang, M. McCumber, R. Adler, and R. Penc, 1990: An algorithm to estimate the heating budget from vertical hydrometeor profiles. *J. Appl. Meteor.,* **29,** 1232–1244, doi:10.1175/1520-0450(1990)029<1232:AATETH>2.0.CO;2.

Testud, J., S. Oury, R. A. Black, P. Amayenc, and X. Dou, 2001: The concept of ''normalized'' distribution to describe raindrop spectra: A tool for cloud physics and cloud remote sensing. *J. Appl. Meteor.,* **40,** 1118–1140, doi:10.1175/1520-0450(2001)040<1118:TCONDT>2.0.CO;2.

Thurai, M., V. N. Bringi, and P. T. May, 2010: CPOL radar-derived drop size distribution statistics of stratiform and convective rain for two regimes in Darwin, Australia. *J. Atmos. Oceanic Technol.,* **27,** 932–942, doi:10.1175/2010JTECHA1349.1.

Tokay, A., and D. A. Short, 1996: Evidence from tropical raindrop spectra of the origin of rain from stratiform versus convective clouds. *J. Appl. Meteor.,* **35,** 355–371, doi:10.1175/1520-0450(1996)035<0355:EFTRSO>2.0.CO;2.

——, P. G. Bashor, E. Habib, and T. Kasparis, 2008: Raindrop size distribution measurements in tropical cyclones. *Mon. Wea. Rev.,* **136,** 1669–1685, doi:10.1175/2007MWR2122.1.

Uijlenhoet, R., M. Steiner, and J. A. Smith, 2003: Variability of raindrop size distributions in a squall line and implications for radar rainfall estimation. *J. Hydrometeor.,* **4,** 43–61, doi:10.1175/1525-7541(2003)004<0043:VORSDI>2.0.CO;2.

Ulbrich, C. W., and L. G. Lee, 2002: Rainfall characteristics associated with the remnants of Tropical Storm Helene in upstate South Carolina. *Wea. Forecasting,* **17,** 1257–1267, doi:10.1175/1520-0434(2002)017<1257:RCAWTR>2.0.CO;2.

Ushiyama, T., K. K. Reddy, H. Kubota, K. Yasunaga, and R. Shirooka, 2009: Diurnal to interannual variation in the raindrop size distribution over Palau in the western tropical Pacific. *Geophys. Res. Lett.,* **36,** L02810, doi:10.1029/2008GL036242.

Varble, A., and Coauthors, 2011: Evaluation of cloud-resolving model intercomparison simulations using TWP-ICE observations: Precipitation and cloud structure. *J. Geophys. Res.,* **116,** D12206, doi:10.1029/2010JD015180.

Waliser, D. E., and Coauthors, 2012: The ''Year'' of Tropical Convection (May 2008 to April 2010): Climate variability and weather highlights. *Bull. Amer. Meteor. Soc.,* **93,** 1189–1218, doi:10.1175/2011BAMS3095.1.

Webster, P. J., and R. Lukas, 1992: TOGA COARE: The Coupled Ocean–Atmosphere Response Experiment. *Bull. Amer. Meteor. Soc.,* **73,** 1377–1416, doi:10.1175/1520-0477(1992)073<1377:TCTCOR>2.0.CO;2.

Wheeler, M. C., and H. H. Hendon, 2004: An all-season real-time multivariate MJO index: Development of an index for monitoring and prediction. *Mon. Wea. Rev.,* **132,** 1917–1932, doi:10.1175/1520-0493(2004)132<1917:AARMMI>2.0.CO;2.

Yuter, S. E., and R. A. Houze, 1995: Three-dimensional kinematic and microphysical evolution of Florida cumulonimbus. Part I: Spatial distribution of updrafts, downdrafts, and precipitation. *Mon. Wea. Rev.,* **123,** 1921–1940, doi:10.1175/1520-0493(1995)123<1921:TDKAME>2.0.CO;2.